The Astrophysical Journal, 579:817–831, 2002 November 10

s-PROCESS NUCLEOSYNTHESIS IN CARBON STARS

C. Abia and I. Domínguez
Departamento de Física Teórica y del Cosmos, Universidad de Granada, E-18071 Granada, Spain; cabia@ugr.es, inma@ugr.es

R. Gallino
Dipartimento di Fisica Generale, Universitá di Torino and Sezione INFN di Torino, via P. Giuria 1, 10125 Torino, Italy; gallino@ph.unito.it

M. Busso
Dipartimento di Fisica, Università di Perugia, via Pascoli, 06123 Perugia, Italy; maurizio.busso@fisica.unipg.it

S. Masera
Dipartimento di Fisica Generale, Università di Torino, via P. Giuria 1, 10125 Torino, Italy; smasera@to.infn.it

O. Straniero
Osservatorio Astronomico di Collurania, I-64100 Teramo, Italy; straniero@astrte.te.astro.it

P. de Laverny
Observatoire de la Cote d'Azur, Departement Fresnel UMR 6528, Nice, France; laverny@obs-nice.fr

B. Plez
Université de Montpellier 2, Montpellier, France; plez@graal.univ-montp2.fr

and

J. Isern
Institut d'Estudis Espacials de Catalunya (CSIC), Barcelona, Spain; isern@ieec.fcr.es
Received 2002 May 24; accepted 2002 July 16

ABSTRACT

We present the first detailed and homogeneous analysis of the *s*-element content in Galactic carbon stars of N type. Abundances of Sr, Y, Zr (low-mass *s*-elements, or ls), Ba, La, Nd, Sm, and Ce (high-mass *s*-elements, or hs) are derived using the spectral synthesis technique from high-resolution spectra. The N stars analyzed are of nearly solar metallicity and show moderate *s*-element enhancements, similar to those found in S stars, but smaller than those found in the only previous similar study (Utsumi 1985), and also smaller than those found in supergiant post–asymptotic giant branch (post-AGB) stars. This is in agreement with the present understanding of the envelope *s*-element enrichment in giant stars, which is increasing along the spectral sequence M → MS → S → SC → C during the AGB phase. We compare the observational data with recent *s*-process nucleosynthesis models for different metallicities and stellar masses. Good agreement is obtained between low-mass AGB star models ($M \lesssim 3\ M_{\odot}$) and *s*-element observations. In low-mass AGB stars, the $^{13}C(\alpha, n)^{16}O$ reaction is the main source of neutrons for the *s*-process; a moderate spread, however, must exist in the abundance of ^{13}C that is burnt in different stars. By combining information deriving from the detection of Tc, the infrared colors, and the theoretical relations between stellar mass, metallicity, and the final C/O ratio, we conclude that most (or maybe all) of the N stars studied in this work are intrinsic, thermally pulsing AGB stars; their abundances are the consequence of the operation of third dredge-up and are not to be ascribed to mass transfer in binary systems.

Subject headings: nuclear reactions, nucleosynthesis, abundances — stars: abundances — stars: AGB and post-AGB — stars: carbon — stars: evolution

1. INTRODUCTION

It is known that the chemical composition of the interstellar medium is oxygen-rich. Hence, the overwhelming majority of the stars are formed with a carbon-to-oxygen ratio lower than unity, and most of them do not change this property during their evolution. However, there are exceptions: several classes of stars are known whose carbon-to-oxygen ratio in the envelope is larger than unity (by number of atoms). These stars are named carbon (C) stars. The existence of carbon stars must be related to some specific mechanism, acting on a limited population of objects. There are basically three possibilities: (1) the carbon enrichment is the result of a deep mixing process suitable to pollute the photosphere with the carbon synthesized by shell He burning in the stellar interior, (2) it is due to mass transfer of carbon-rich material after the stellar birth, or (3) it dates back to the star's birth, as the result of an anomalous composition of the parental cloud, more enriched in carbon than in oxygen. Concerning the last hypothesis, so far no such interstellar clouds have been detected in Galactic disk environments, although the hypothesis is not completely ruled out for certain low-metallicity stars (Beveridge & Sneden 1994). In the second case, the origin of the carbon-rich material is simply moved to another place, i.e., the carbon-rich primary component of a binary system. For instance, the stars of the CH spectral type (Luck & Bond 1991; Vanture 1992a, 1992b, 1992c) most likely owe their carbon enhancement to the transfer of carbon-rich material from a companion (now a white dwarf). These stars are usually named *extrinsic* asymptotic giant branch (AGB) stars to distinguish them from those deriving their carbon enhancement from nuclear

processing in their interiors (hypothesis 1), which are called *intrinsic*. Here we shall deal with a specific subclass of carbon stars, those of spectral type N. We shall see later that most probably all of them can be classified as intrinsic C-rich objects. They are formed through the mixing into the envelope of newly produced ^{12}C from He burning. Stellar evolution then limits the candidates to evolved stars with masses $1 \lesssim M/M_{\odot} \lesssim 8$, in particular those ascending the AGB. The structure of an AGB giant is characterized by a degenerate CO core, by two shells (of H and He) burning alternatively, and by an extended convective envelope. In the H-R diagram, these stars lie close to the brightest part of the Hayashi line. They become long-period variables of the irregular, semiregular, or Mira types, presenting large mass-loss rates: 10^{-8} to 10^{-4} $M_{\odot}$ yr^{-1} (Wallerstein & Knapp 1998). As a consequence, a thick circumstellar envelope eventually forms, sometimes developing detached shells. Depending on its chemical composition and optical thickness, this circumstellar material can obscure partially or completely the central star at optical wavelengths (Knapp & Morris 1985; Olofsson et al. 1993; Marengo, Ivezic, & Knapp 2001). Schwarzschild & Härm (1965) early showed that thermal instabilities in the He shell (thermal pulses [TPs]) occur periodically during the advanced phases of AGB evolution. During a TP the whole region between the H shell and the He shell (called "the He intershell") becomes convective. After a number of TPs, the convective envelope penetrates downward, dredging up material previously exposed to incomplete He-burning conditions. This phenomenon is called *third dredge-up* (TDU), and its main consequence is the increase of the carbon content in the envelope so that, eventually, the C/O ratio can exceed unity and the star may become a carbon star. In such a way, the carbon content in the envelope is expected to increase along the spectral sequence M $\rightarrow$ MS $\rightarrow$ S $\rightarrow$ SC $\rightarrow$ C, stars of spectral class C showing C/O > 1 (see, e.g., Iben & Renzini 1983; Smith & Lambert 1990).

Another important consequence of TDU is the enrichment of the envelope in *s*-elements. The necessary neutrons for the *s*-process are released by two reactions: $^{13}C(\alpha, n)^{16}O$, which provides the bulk of the neutron flux at low neutron densities ($N_n \lesssim 10^7$ cm^{-3}), and $^{22}Ne(\alpha, n)^{25}Mg$, which is activated at temperatures $T \gtrsim 3.0 \times 10^8$ K, providing a high peak neutron density ($N_n \sim 10^{10}$ cm^{-3}), and is responsible for the production of *s*-nuclei controlled by reaction branchings (see Wallerstein et al. 1997; Busso, Gallino, & Wasserburg 1999 and references therein). The abundances of *s*-nuclei are known to increase along the above-mentioned spectral sequence, as the star gradually ascends the AGB. Evidence of this was provided during the last few decades by several studies on AGB stars of different spectral types: MS and S stars (C/O < 1; Smith & Lambert 1985, 1986, 1990), SC stars (C/O ~ 1; LLoyd-Evans 1983; Abia & Wallerstein 1998, hereafter Paper I), and even post-AGB supergiants of spectral types A and F (Van Winckel & Reyniers 2000; Reddy, Bakker, & Hrivnak 1999).

The above studies found consistent enhancements of *s*-elements with respect to "normal" red giants assumed as comparisons (or with respect to the Sun): from $[s/\mathrm{Fe}] \approx 0.3$ in MS giants to $[s/\mathrm{Fe}] > 0.5$ in S stars.[1] The enrichment seems to continue along the AGB phase until the planetary nebula ejection. Indeed, post-AGB supergiants show high enhancements, $[s/\mathrm{Fe}] > 1.0$. In this scenario, however, normal carbon stars (N type[2]) still have to find a place. This is so because of the complex spectra of N stars, which are so crowded with molecular and atomic absorption features (many of which are unidentified) that abundance analysis has been strongly limited.

The situation has not improved much with the advent of spectrum synthesis techniques. Indeed, the only abundance studies available to date are those by Kilston (1975) and Utsumi (1970, 1985), still based on abundance indexes and on low-resolution photographic spectra, respectively. These works suggested that N stars were *s*-element–rich, showing overabundances by a factor of 10 with respect to the Sun. As far as the AGB phase is concerned, this figure is not in direct contradiction with the accepted general scenario of *s*-nuclei enhancement (see, e.g., Busso et al. 1995). More likely, such high production factors might be difficult to reconcile with the enrichment in post-AGB supergiants showing similar, or even smaller, abundances. However, the large observational uncertainties for C-rich red giants and the lack of adequate model atmospheres have so far prevented a solid theoretical interpretation.

In a previous work (Abia et al. 2001, hereafter Paper II) we presented high-resolution spectroscopic observations for a sample of N stars, focusing our attention on light *s*-elements (ls), sited at the abundance peak near the neutron magic number $N = 50$, around the ^{85}Kr branching point of the *s*-process path. We showed how the analysis of the abundance ratios of Rb (a neutron density–sensitive element; see, e.g., Beer & Macklin 1989) relative to its neighbors (Sr, Y, and Zr) yields information on important details of the *s*-process mechanism operating and on the initial stellar mass. We concluded that *s*-processing suggests low-mass stars (LMSs; $M \lesssim 3$ $M_{\odot}$) as the likely parents of C(N) giants.

In LMSs the major neutron source is ^{13}C, which burns radiatively in a tiny layer during the interpulse phase (Straniero et al. 1995) at relatively low temperatures ($\approx$8 keV), as a consequence of the formation of a ^{13}C-rich *pocket* in the intershell region. In the rarer AGB intermediate-mass stars (IMSs; $M \gtrsim 4$ $M_{\odot}$), ^{22}Ne would instead be favored as a neutron source, by the higher temperature in thermal pulses. Because of the very different neutron density provided by the two neutron-producing reactions, different compositions are expected from them, especially for the ls mixture. It is on this basis that in Paper II we drew our conclusions for the initial masses.

In Paper II we also discussed the $^{12}C/^{13}C$ ratios measured in the sample stars, showing that most of them cannot be explained by canonical stellar models on the AGB phase, requiring probably the operation of an ad hoc mixing mechanism. This mechanism is often indicated with the term "cool bottom process" (CBP). It is expected to occur in low-mass stars during the red giant branch (RGB) and perhaps also during the AGB phase (Wasserburg, Boothroyd, & Sackmann 1995; Nollett, Busso, & Wasserburg 2002).

[1] We adopt the usual notation $[\mathrm{X/Y}] \equiv \log(\mathrm{X/Y})_{\mathrm{program\,star}} - \log(\mathrm{X/Y})_{\mathrm{comparison\,star}}$ for the stellar value of any element ratio X/Y.

[2] There are carbon stars of R type and J type, which probably owe their carbon enhancement to a mechanism different than the TDU. These stars are not significantly enhanced in *s*-elements (Dominy 1985; Abia & Isern 2000).

In the present work we have extended our study of *s*-element nucleosynthesis in N stars to the nuclei belonging to the second *s*-process peak: Ba, La, Ce, Nd, and Sm. We also reanalyzed the *s*-element abundances already derived in Paper II by applying the spectral synthesis method. Together, these data are compared with recent models for *s*-processing in AGB stars at the metallicities relevant for our sample stars. Furthermore, using the infrared properties and Tc content, we discuss the possibility that our stars are extrinsic carbon stars, concluding that this is unlikely for several reasons. The structure of the paper is as follows. In § 2 we present the characteristics of the stars and the spectroscopic observations. In § 3 we describe the method of analysis and the sources of error. Our abundance results are reported in § 4 together with a comparison with similar studies on other AGB stars and with models of AGB nucleosynthesis. Finally, in § 5 we summarize the main conclusions that can be drawn from this work.

2. OBSERVATIONS AND ANALYSIS

The spectra of our N star sample were collected at the Roque de los Muchachos (ORM) and Calar Alto (CAHA) observatories in several observational runs between 1998 and 2001. In the former case we used the 4.2 m William Herschel Telescope (WHT) and the 2.5 m Nordic Optical Telescope (NOT) with the UES and SOFIN spectrographs, respectively. The UES gives a maximum resolution of about 50,000 between $\lambda = 450$ and 900 nm, with some gaps between orders. SOFIN, working with the third camera configuration, reaches a maximum resolution of 180,000 in 28 orders, covering about the same spectral range but with larger gaps between orders. At the CAHA observatory we used the 2.2 m telescope with the FOCES spectrograph, which provides a resolution of about 35,000 between $\lambda = 360$ and 1000 nm. In this case, an almost complete spectral coverage is obtained. Table 1 shows the sample stars and the epoch of the observations. Data reduction was performed following the standard procedures using the IRAF software package. Details on this are quoted in Abia & Isern (2000) and Paper II. In the present work we add new N stars to the sample studied in Paper II, namely, RV Cyg, S Aur, SS Vir, T Dra, TT Cyg, U Hya, U Lyr, VY UMa, V429 Cyg, and W CMa.

2.1. *Stellar Parameters and Luminosities*

The main parameters of the stars were derived in a way similar to that of Paper II; they will not be discussed again here (see that paper for details). For all the stars we adopted a typical gravity of $\log g = 0.0$ and a microturbulence of $\xi = 2.2$ km s^{-1}. As in previous works, we used the grid of model atmospheres for carbon stars computed by the Uppsala group (see Eriksson et al. 1984 for details). The absolute abundances of CNO, the C/O ratio (which mainly determines the global shape of the spectrum in carbon stars), and the $^{12}C/^{13}C$ ratios were derived as discussed in Paper II. Table 2 shows the final parameters adopted for each star.

In order to estimate the absolute bolometric magnitudes M_{bol} of our stars (Table 1), we used the empirical relationships between M_{bol} and M_K for carbon stars obtained by Alkniss et al. (1998). The average K magnitude values (the stars studied are variable!) were taken from the Two Micron All Sky Survey (Neugebauer & Leigthon 1969), available at the SIMBAD database. Actually, although recent catalogs of near-infrared images and point sources have become available (namely, 2MASS, Skrutskie et al. 1997; DENIS, Epchtein et al. 1999), our sources are too bright for them and are saturated. Recent observations at infrared wavelengths have been collected by Gezari, Pitts, & Schmitz (1999); a few of our stars are present in the compilation, and the colors derived are compatible with those used here within the uncertainties. K magnitudes were corrected for interstellar extinction according to the Galactic extinction model by Arenou, Grenon, & Gómez (1992) with $A_K/A_V = 0.126$ (Cardelli, Clayton, & Mathis 1989). Distances were calculated from the *Hipparcos* intermediate astrometric data (van Leeuwen & Evans 1998). The *Hipparcos* parallaxes for carbon stars generally show much lower precision than those calculated for hotter main-sequence stars. Parallaxes for carbon stars of different spectral types have been partially reprocessed (Knapp, Pourbaix, & Jorissen 2001; Pourbaix, Knapp, & Jorissen 2002; Bergeat, Knapik, & Rutily 2001, 2002a, 2002b). However, the bolometric magnitudes showed in Table 1 still have to be taken with some caution. In any case, it is remarkable that the overwhelming majority of the stars have $M_{bol} \lesssim -7.1$, the maximum theoretical luminosity of an AGB star when its core mass reaches the Chandrasekhar mass limit, according to the core-luminosity relation by Paczyński (1970). Our sample stars have on average $M_{bol} \sim -5$, but a considerable number have lower luminosity. This figure coincides with recent luminosity studies of carbon stars in the Galaxy (Bergeat et al. 2002a) and in the nearby stellar systems (Westerlund et al. 1991, 1995).

2.2. *The List of Lines*

Utsumi (1970) first noted that in N stars the blend effect of molecular bands is not very serious in the spectral regions $\lambda \approx 4400$–4500 and 4750–4950 Å. He also found that many lines of *s*-process and rare earth elements present in these spectral regions are of moderate intensity, and therefore they are useful for abundance analysis. Here, however, we have concentrated our analysis in the $\lambda = 4750$–4950 Å spectral range since the radiation flux received from many carbon stars below 4500 Å is very limited because of the presence of strong C_3 molecular absorption features below that wavelength limit. In Papers I and II we used the equivalent width versus curve-of-growth technique to derive heavy-element abundances through a careful identification and selection of the lines (see these papers for details). In the present study, however, we decided to use the spectral synthesis technique because most of the lines from *s*-elements with high atomic mass (Ba, La, Ce, Nd, and Sm, i.e., hs elements) present in this spectral range are heavily blended. This also allows us to verify the results of Paper II for the ls elements (Sr, Y, Zr), rederiving their abundances independently. This check confirmed the abundances deduced in Paper II (within the error bars, with the exception of a few cases, for reasons that are discussed below). This gives an important confirmation of the previous analysis technique.

The spectral window studied, while being less affected by molecular blends than others, is nevertheless not free from such problems. Lines from the C_2, CH, and CN molecules have therefore to be considered. Transitions from the $^{12}C_2$, $^{12}C^{13}C$, and $^{13}C_2$ (A–X), (B–A), (D–A), and (E–A) systems

TABLE 1
THE PROGRAM STARS

Star	Spectral Type[a]	Variable Type[a]	Period[a] (days)	M_{bol}[b]	Epoch (JD +2,450,000)	Observatory[c]
AQ And	C5,4	SR	346	−5.2	791	CAHA
AW Cyg	C3,6	SRb	220	−5.7	947	ORM
					1745	CAHA
EL Aur	C5,4	Lb	...	−2.5	791	ORM
HK Lyr	C6,4	Lb	...	−6.0	947	ORM
					1015	CAHA
IRC −10397	N	...	...	...	1015	CAHA
					1745	CAHA
IY Hya	N	Lb	...	−5.2	947	ORM
LQ Cyg	C4,5	Lb	...	...	1745	CAHA
RV Cyg	C6,4	SRb	263	−7.1	1745	CAHA
RX Sct	C5,2	Lb	...	...	1015	CAHA
S Aur	C5,4	SR	590	...	745	CAHA
S Sct	C6,4	SRb	148	−4.6	1015	CAHA
SS Vir	C6,3	SRa	364	...	1745	CAHA
SY Per	C6,4	SRa	476	−3.1	791	CAHA
SZ Sgr	C7,3	SRb	100	−2.1	1015	CAHA
T Dra	C6,2	Mira	421	−2.0	791	CAHA
TT Cyg	C5,4	SRb	118	−4.6	1015	CAHA
					1745	CAHA
TY Oph	C5,5	Lb	...	...	1015	CAHA
U Cam	C3,9	SRb	400	−4.8	791	ORM
U Hya	C6,3	SRb	450	−4.0	947	ORM
					1919	ORM
U Lyr	C4,5	Mira	457	−5.5	791	CAHA
UU Aur	C5,3	SRb	235	−6.0	947	ORM
UV Aql	C6,2	SRa	385	−7.0	947	ORM
					1745	CAHA
UX Dra	C7,3	SRa	168	−5.6	947	ORM
V Aql	C6,4	SRb	353	−5.0	1745	CAHA
V CrB	C6,2	Mira	357	−7.1	1015	CAHA
					947	ORM
V Oph	C5,2	Mira	298	−5.9	1015	CAHA
					947	ORM
VX Gem	C7,2	Mira	379	−3.6	745	CAHA
					1919	ORM
VY UMa	C6,3	Lb	...	−4.3	1919	ORM
V429 Cyg	C5,4	SRa	164	...	745	CAHA
					1745	CAHA
V460 Cyg	C6,3	SRb	180	−5.8	1015	CAHA
					1745	CAHA
V781 Sgr	N	Lb	...	...	1015	CAHA
W CMa	C6,3	Lb	...	−7.3	1919	ORM
W Ori	C5,4	SRb	186	−5.6	791	CAHA
WZ Cas	C9,2J	SRa	186	−6.2	745	CAHA
					791	ORM
					1919	ORM
Z Psc	C7,2	SRb	144	−4.1	745	ORM

[a] Data taken from the SIMBAD database.
[b] Bolometric magnitudes are estimated from mean *K* magnitudes and *Hipparcos* parallaxes (see text).
[c] CAHA: Centro Astronómico Hispano-Alemán de Calar Alto; ORM: Observatorio del Roque de los Muchachos.

were found in the Kurucz database.[3] From the work of de Laverny & Gustafsson (1998) and Kurucz data, no C_2 lines from the Phillips red system were predicted to be of importance in the studied spectral ranges. $^{12}C^{14}N$, $^{13}C^{14}N$, $^{12}C^{15}N$, and $^{13}C^{15}N$ lines were included. The CN line lists were prepared along the same lines as the TiO line list of Plez (1998), using data from Ito et al. (1988), Kotlar, Field, & Steinfeld (1980), Cerny et al. (1978), Rehfuss, Suh, & Miller (1992), Prasad & Bernath (1992), Prasad et al. (1992), Bauschlicher, Langhoff, & Taylor (1988), and Larsson, Siegbahn, & Ågren (1983). Programs by Kotlar were used to compute wavenumbers of transitions in the red bands studied by Kotlar et al. (1980). Lines from the violet system were found to be very weak but were nevertheless considered. The absorption by the C_2, $^{13}C^{15}N$, $^{12}C^{15}N$, and $^{13}C^{14}N$ lines is found to slightly decrease the theoretical continuum by a few percent without affecting the line depths. In that

[3] Available at http://cfaku5.harvard.edu/linelists.html.

TABLE 2
DATA FOR PROGRAM STARS

Star	$T_{\rm eff}$	Reference[a]	C/O	$^{12}C/^{13}C$	Reference[b]	K–[12][c]	K–[25][c]
AQ And	2970	1	1.02	30	1	−1.80	−3.16
AW Cyg	2760	1	1.03	21	2	−1.59	−2.92
EL Aur	3000	2	1.07	50	2	−1.64	−2.83
HK Lyr	2866	1	1.02	10	2	−1.92	−3.18
IRC −10397	2600	2	1.01	20	2	...	...
IY Hya	2500	2	1.02	15	2	5.61	...
LQ Cyg	2620	1	1.10	40	2	−1.98	−3.19
RV Cyg	2600	3	1.20	74	3	−2.87	−1.59
RX Sct	3250	1	1.04	60	2	...	...
S Sct	2895	3	1.07	45	3	−1.92	−3.32
SS Vir	2560	4	1.05	10	2	−2.60	−1.34
SY Per	3070	5	1.02	43	2	−1.69	−2.86
SZ Sgr	2480	1	1.03	8	2	−1.74	−2.43
TT Cyg	2825	4	1.04	30	2	−3.50	−2.05
TY Oph	2780	1	1.05	45	2	−1.89	−2.95
U Cam	2670	1	1.02	40	2	−1.44	−2.57
U Hya	2825	3	1.05	35	2	−3.00	−1.86
UU Aur	2825	3	1.06	50	3	−1.80	−3.06
UV Aql	2750	1	1.005	19	2	−1.74	−3.06
UX Dra	2900	3	1.05	26	2	−2.30	−3.58
V Aql	2610	3	1.16	90	2	−1.74	−3.17
V CrB	2250	6	1.10	10	4	0.02	−1.24
V Oph	2880	1	1.05	11	1	−1.64	−2.96
VX Gem	2500	7	1.01	60	2	−1.46	−2.93
VY UMa	2855	3	1.08	44	3	−3.56	−2.13
V460 Cyg	2845	3	1.06	61	3	−2.05	−3.43
V781 Sgr	3160	1	1.02	35	3	−3.22	−1.86
W CMa	2880	3	1.09	53	3	−2.92	−1.98
W Ori	2680	3	1.20	79	3	−3.04	−1.69
WZ Cas	3140	5	1.005	4	3	−3.66	−2.39
Z Psc	2870	3	1.01	55	3	−3.55	−2.39

[a] References for $T_{\rm eff}$: (1) Ohnaka & Tsuji 1996; (2) for these stars we have estimated the effective temperature by comparing their spectra with the temperature sequence spectral atlas for C stars created by Barnbaum, Stone, & Keenan 1996; (3) Lambert et al. 1986; (4) Bergeat et al. 2001; (5) Dyck, van Belle, & Benson 1996; (6) Kipper 1998; (7) Groenewegen et al. 1998.

[b] Source for the $^{12}C/^{13}C$ ratio: (1) Ohnaka & Tsuji 1996; (2) derived in this work or Paper II; (3) Lambert et al. 1986; (4) Kipper 1998.

[c] The 12 and 25 μm fluxes are taken from the 2d ed. of the *IRAS* PSC and the K magnitudes from the Two Micron All Sky Survey indicated in Claussen et al. 1987.

spectral range, the main contributor from these two molecules is $^{12}C^{14}N$. We adopted a solar $^{15}N/^{14}N$ in all the spectral synthesis. Several CH lines also play a role in the 4750–4950 Å spectral range. The LIFBASE program of Luque & Crosley (1999) was used to compute these line positions and *gf*-values. Excitation energies and isotopic shifts (LIFBASE provides only line positions for ^{12}CH) were taken from the line list of Jørgensen et al. (1996). In this way, a very good fit of CH lines in the solar spectrum could be obtained, with the exception of very few lines, which we removed from the list. Obviously, the line list also comprises atomic line data found in the VALD database (Kupka et al. 1999) and in Kurucz's (1993) data, although for the more intense atomic lines (mostly metals) we derived solar *gf*-values using the Holweger & Müller (1974) model atmosphere and solar abundances by Anders & Grevesse (1989). The *gf*-values derived in such a way showed an excellent agreement with the solar values derived by Thévenin (1989, 1990). For a sample of about 100 lines in common we found a mean difference of 0.15 ± 0.2 dex. Our final line list includes more than 20,000 atomic and molecular lines. Despite this, only a few lines were selected as indicators of the hs element abundances in our stars. These lines are shown in Table 3. The metallicity [M/H] of our sample stars was derived from selected metallic lines, "M" indicating an average value of Ca, Ti, V, Fe, and Co abundances (see Table 3 in Paper II). Using this average changes only slightly the values of [ls/Fe] and [hs/Fe] derived.

2.3. *Data Analysis, Peculiar Cases, Comparison with Previous Work*

The hs element abundances were derived from spectrum synthesis fits to the observed spectra. The theoretical spectra were computed in LTE, and the abundance analysis was done line by line relative to the star WZ Cas (C9,2J;SC7/10), which was used, as in Paper II, as the reference star. WZ Cas is a carbon star with a C/O ratio very close to unity with nearly solar metallicity and with very small or no *s*-element enhancement: $[h/{\rm Fe}] = 0.02 \pm 0.20$, where h (heavies) includes Sr, Y, Zr, Nb, Ba, La, Ce, and Pr (see Lambert et al. 1986; Abia & Isern 2000). This comparative analysis might reduce systematic errors due to wrong *gf*-values and possible departures from LTE (Tomkin & Lambert 1983).

TABLE 3
SPECTROSCOPIC DATA

Line	χ (eV)	log gf	Reference
Ba II λ4934.10	0.00	−0.150[a]	1
La II λ4804.04	0.23	−1.530	2
La II λ4809.02	0.23	−1.267	3
La II λ4748.73	0.93	−0.600	3
Ce II λ4773.96	0.92	0.010	4
Ce I λ4820.00.....	0.27	−0.559	5
Ce I λ4820.61.....	0.17	−0.866	5
Ce I λ4822.54.....	0.00	−0.420	5
Nd II λ4811.35.....	0.06	−0.570	6
Nd II λ4817.18.....	0.74	−0.760	2
Nd II λ4825.48.....	0.18	−0.880	2
Nd II λ4832.27.....	0.56	−0.920	2
Sm II λ4777.85.....	0.04	−1.340	2
Sm II λ4815.80.....	0.18	−0.770	2

[a] Hyperfine structure included according to McWilliam 1998.

REFERENCES.—(1) McWilliam 1998. (2) VALD database (Piskunov et al. 1995). (3) Bard, Barisciano, & Cowley 1996. (4) Thévenin 1989. (5) Meggers, Corliss, & Scribner 1975. (6) Solar gf derived.

All the abundance ratios derived (see below) are relative to this star. The final abundance derived for each element is the mean of the abundances derived from each line, except for Ba, whose abundance is derived from only one line. In deriving these means, we consider twice the abundances derived from particular lines that we believe are better abundance indicators for a given element because of their larger sensitivity to abundance variations and/or because they are placed in a less crowded region. These lines are La II λ4809, Ce II λ4773, and Nd II λ4811 (see Table 3).

Figure 1 shows an example of a theoretical fit to the observed spectrum of the star Z Psc in the 4800–4830 Å region, where most of the available *s*-element lines are located. Figure 2 is a similar example in the region around the Ba II λ4934 line. It can be seen in both figures that the observed spectra are generally well fitted by spectral synthesis, despite the fact that many features are still not accounted for. This last fact is clear evidence of the remaining incompleteness of the line list used, despite the several thousands of lines included.

As noted above, in the present work we have rederived with the spectral synthesis technique the abundances of Sr, Y, and Zr obtained in Paper II; this was permitted by the fact that most of the available lines for these elements are located in the same spectral range 4750–4950 Å studied here (see Table 3 in Paper II). We find a good agreement (within typical error bars) with the values found for these elements in Paper II; hence, our conclusions are not modified by the present analysis. Only for one star, V460 Cyg, are the abundances of Sr, Y, and Zr significantly modified. The reason for this arises from a bad interpolation done in Paper II over the grid of model atmosphere parameters for this star. There is also a modification of the Rb and Zr abundances in Z Psc with respect to Paper II. The Rb abundance shown there (Table 2) is just a misprint, the correct value being [Rb/M] = 0.6 instead of 0.9. The revised [Zr/M] ratio here is 1.0 dex, which is, nevertheless, in agreement within error bars with the previous value in Paper II (0.8 dex). In the

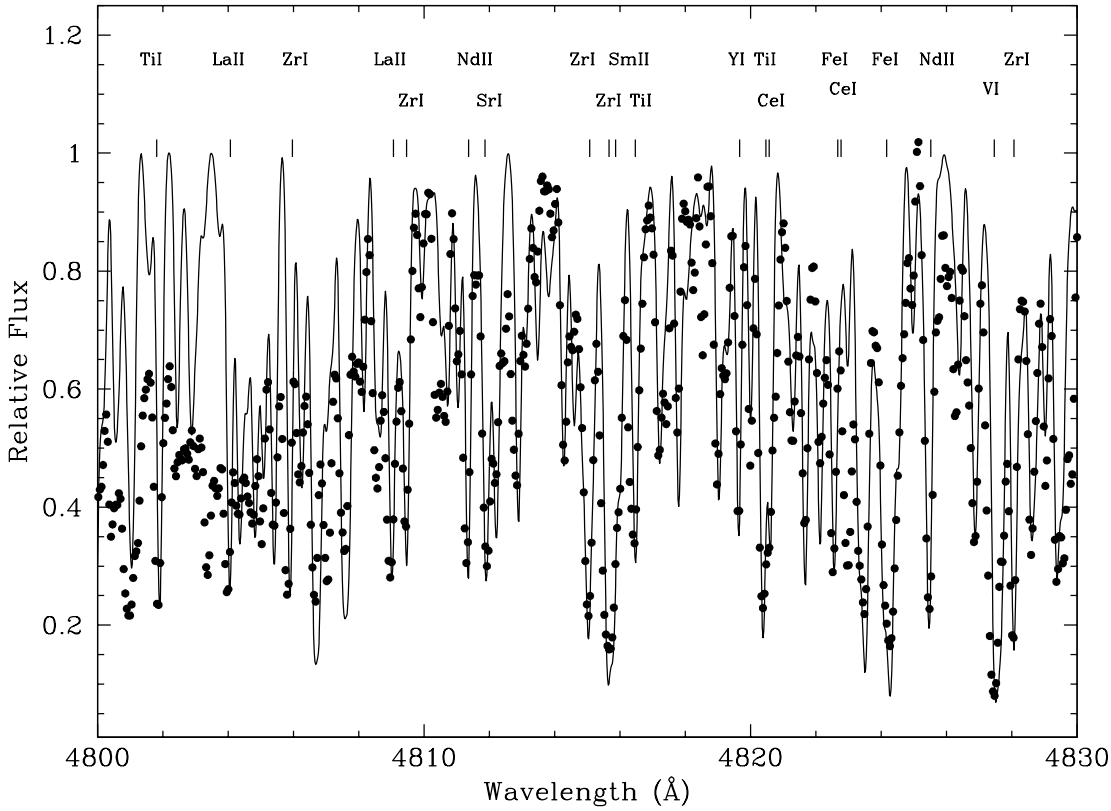

FIG. 1.—Best synthetic fit (*solid line*) to the observed (*filled circles*) spectrum of the star Z Psc in the range 4800–4830 Å. The main atomic absorption lines are indicated. Note that there are still many spectral features not well reproduced by our synthetic spectrum.

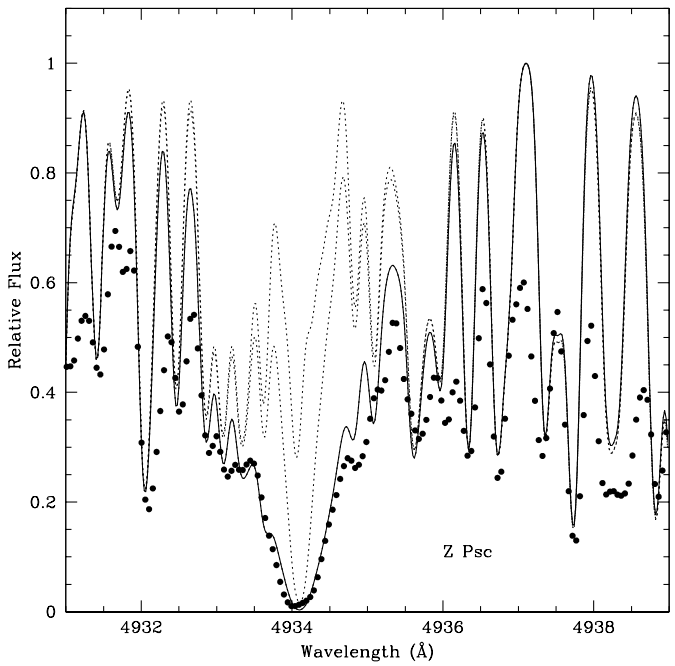

FIG. 2.—Same as Fig. 1, but for the star in the region of the Ba II λ4934 line for different Ba abundances: no Ba (*upper dashed line*), $12 + \log(\mathrm{Ba/H}) = 2.13$ and 3.1 (best fit, *solid line*).

present work we have also been able to estimate the Sr abundance in this star using the Sr I λ4811.88 line: we recall that the Sr abundance in Z Psc was not derived in Paper II.

In Paper II we also discussed the increased difficulties found in the analysis of certain N stars, in particular IY Hya, VX Gem, and V CrB (see that paper for details). In fact, the abundance results in such stars were considered with a lower weight in comparing with theoretical models. Unfortunately, here the list of *difficult* stars has to be extended. Indeed, T Dra, U Lyr (both Mira variables), S Aur, and V429 Cyg show spectra so smeared out that we had no choice but to decide to give up their analysis. For SS Vir and V Oph (also Mira variables), the spectra are also smeared out, and in fact they provide an insufficient agreement between observed and theoretical spectra. In particular, all Mira variables in our sample show difficult spectra. It is not clear why spectral lines in the Mira variables look this way. Mira variables generally have thick circumstellar dust shells, whose contamination due to thermal emission by dust might be responsible for this problem. The gas motions due to pulsation might contribute to the broadening of spectral lines. Finally, the star V781 Sgr shows a weak central emission at the core of the Na D lines. This is usually interpreted as due to the presence of a chromosphere. The influence of a chromosphere in the derivation of abundances in carbon stars is uncertain and is beyond the scope of this work; therefore, we have included also this star in the group of *difficult* N stars. Summing up, the abundances derived for IY Hya, VX Gem, V CrB, SS Vir, V Oph, and V781 Sgr have to be considered with considerable caution. To emphasize this, in the figures below, we have plotted with smaller symbols the abundance ratios derived for them.

The stellar atmosphere parameters ($T_{\rm eff}$, gravity, etc.) for N stars are difficult to determine with accuracy (Bergeat et al. 2001, 2002a). Note for instance that they are variable stars; therefore, the effective temperature changes during the pulsation. The microturbulence in variable stars depends on the wavelength in the spectrum (as a result of differences in depth of formation) and changes with the pulsational phase. Furthermore, the existence of strong waves, shock fronts, and inhomogeneities is the rule rather than the exception in their atmosphere (see Gustafsson & Jørgensen 1994 for discussion). In Table 4 we show the sensitivity of the abundances derived to typical uncertainties in the atmosphere parameters. Since most of the lines used in the present work correspond to singly ionized elements (see Table 3), an important source of uncertainty is the error in the gravity. The abundances derived are rather sensitive to the microturbulence parameter, indicating some saturation of the lines used in the analysis. However, the hs element abundances are mostly insensitive to uncertainties in metallicity, CNO absolute abundances, and the $^{12}C/^{13}C$ ratio. Certainly, deviations from LTE might play a significant role, although they are reduced in a differential analysis as is done here. If we consider the uncertainty due to the placement of the spectral continuum ($\sim$5%), adding quadratically all the sources (nonsystematic) of error, we find a typical uncertainty in the absolute abundances of about $\pm$0.2 dex for Ba, $\pm$0.4 dex for La, Nd, and Sm, and $\pm$0.45 dex for Ce.

Furthermore, we have to consider the random error in the abundances of elements represented only by a few lines, as in our case. We can estimate this random error only in stars where we derived individual element abundances from more than three lines. In this case we found a dispersion in the range 0.1–0.3 dex. Nevertheless, when computing the [hs/M] ratios, errors are lower because some sources of error affect in the same way the metallicity (see Table 4 in Paper II). Adding up all these contributions, we estimate a typical total error (nonsystematic) in the [hs/M] ratios ranging from $\pm$0.3 (Ba) to $\pm$0.45 dex (Ce). A similar discussion can be had concerning the uncertainties in the derivation of the ls element abundances and metallicity (see Paper II for details). Considering this, we estimate a typical error of about $\pm$0.3 dex in the [hs/ls] ratios. In Table 5 we show the abundance ratios with respect to the metallicity derived in

TABLE 4
DEPENDENCE OF DERIVED ABUNDANCES ON MODEL ATMOSPHERE PARAMETERS

Abundance	$\Delta T_{\rm eff} = \pm 200$ K	$\Delta \log = \pm 0.5$	$\Delta\xi = \pm 0.5$ km s^{-1}	ΔC/O = $\pm$0.05	$\Delta^{12}C/^{13}C = \pm 10$	ΔCNO/H = $\pm$0.2	Δ[M/H] = $\pm$0.3
[Ba/H]	$\pm$0.02	$\pm$0.15	$\mp$0.05	$\pm$0.10	$\pm$0.0	$\pm$0.01	$\pm$0.05
[La/H]	$\pm$0.0	$\pm$0.20	$\mp$0.30	$\pm$0.10	$\pm$0.0	$\pm$0.01	$\pm$0.10
[Ce/H]	$\pm$0.05	$\pm$0.30	$\mp$0.40	$\pm$0.10	$\pm$0.0	$\mp$0.10	$\pm$0.10
[Nd/H].....	$\pm$0.02	$\pm$0.20	$\mp$0.40	$\pm$0.10	$\pm$0.0	$\mp$0.10	$\pm$0.05
[Sm/H].....	$\pm$0.0	$\pm$0.20	$\mp$0.40	$\pm$0.0	$\pm$0.0	$\pm$0.01	$\pm$0.10

TABLE 5
ABUNDANCES DERIVED IN PROGRAM STARS

Star	[M/H]	[Rb/M]	[Sr/M]	[Y/M]	[Zr/M]	[Ba/M]	[La/M]	[Ce/M]	[Nd/M]	[Sm/M]	Tc
AQ And	0.02	0.3	0.6	0.7	0.5	0.1	0.1	...	0.3	0.0	No
AW Cyg	0.0	0.2	0.4	0.3	0.5	0.0	0.3	...	<0.5	...	Yes
EL Aur	−0.06	0.4	0.5	0.7	0.8	0.2	0.2	0.1	0.2	...	No
HK Lyr	−0.10	0.2	0.3	0.8	0.7	0.8	0.8	...	0.7	...	Yes
IRC −10397	0.10	0.1	0.3	...	...	...	...	...	...	...	No
IY Hya	−0.80	0.5	0.6	<0.7	<0.7	<0.5	...	...	...	...	...
LQ Cyg	0.25	0.2	<0.5	0.8	0.7	0.4	0.4	...	0.5	<0.4	No
RV Cyg	0.0	...	0.0	0.3	...	0.0[a]	...	...	...	...	No
RX Sct	−0.05	0.4	0.4	0.7	0.8	0.7	0.7	...	0.8	<0.5	No
S Sct	0.01	0.5	0.8	0.7	0.5	0.2	0.1	...	0.2	...	Yes
SS Vir	0.0	...	0.0	0.5	0.4	0.3	0.4	...	0.3	...	Doubtful
SY Per	−0.30	0.1	0.5	...	...	...	...	...	...	...	Doubtful
SZ Sgr	−0.04	0.1	0.4	0.9	0.8	0.8	0.9	...	0.9	<0.6	Doubtful
TT Cyg	−0.1	...	...	1.2	1.0	0.8	0.9	...	0.9	<0.6	Doubtful
TY Oph	0.10	0.2	0.6	0.7	0.6	0.6	0.5	...	0.6	...	Doubtful
U Cam	−0.09	...	...	0.8	0.5	0.5[a]	0.5	0.2	0.5	0.3	No
U Hya	−0.05	0.5	0.8	1.3	1.1	1.1	0.9	0.6	<1.0	<0.7	Yes
UU Aur	0.06	0.4	0.4	0.6	0.6	0.3	0.2	...	0.3	<0.2	No
UV Aql	−0.06	0.6	0.5	0.7	0.9	0.6	0.6	...	0.7	...	Yes
UX Dra	−0.20	0.0	0.8	0.8	0.7	0.7	0.4	...	0.4	...	Yes
V Aql	−0.05	0.3	0.5	...	...	0.2[a]	...	...	...	...	No
V CrB	−1.35	−0.2	0.3	0.4	...	...	...	...	...	...	No
V Oph	0.0	−0.2	0.2	0.3	0.4	0.1	0.1	−0.05	0.2	...	...
VX Gem	−0.15	...	0.6	0.5	0.6	0.8	...	<1.0	...	<1.0	Yes
VY UMa	−0.1	0.3	0.5	0.8	1.1	...	1.0	...	0.8	<0.6	Yes
V460 Cyg	−0.04	0.4	0.5	0.7	0.8	0.8	0.7	...	0.8	<0.4	Yes
V781 Sgr	0.10	0.1	0.5	0.3	0.3	0.1	0.2	...	0.1	...	Yes
W CMa	0.0	0.2	0.6	...	...	...	...	...	...	...	...
W Ori	0.05	...	0.0	0.3	0.2	0.3	0.3	...	0.1	...	No
Z Psc	−0.01	0.6	0.9	1.0	1.0	1.0	1.1	0.6	0.9	0.8	Yes

[a] The stars RV Cyg, U Cam, and V Aql show weak Merill-Sanford (SiC_2) band absorptions not included in the analysis that could affect the derivation of the Ba abundance.

our stars, referred to the comparison star WZ Cas. The abundances in Table 5 represent the first detailed analysis of the *s*-element composition in N stars. In this table we show the previous results (revised) obtained in Paper II for the ls elements, together with the new values derived here for the hs elements, including some additional stars (see § 2). We confirm our previous finding that N stars are of nearly solar metallicity: $\langle[M/H]\rangle = -0.02 \pm 0.10$. Only two stars seem to be of low metal content (IY Hya and V CrB); however, we remind the reader of the difficulties found in the analysis of these objects (see above). Considering the abundances of Y and Zr as the only good tracers of the ls element enhancement,[4] our objects have $\langle[ls/M]\rangle = 0.67 \pm 0.24$. In the same way, considering Ba, La, and Nd as representative of the hs element enhancement (Ce and Sm are derived only in a few stars; in many of them we set just upper limits), the mean is $\langle[hs/M]\rangle = 0.52 \pm 0.29$. This figure represents moderate but significant *s*-element enhancement, which is clearly smaller than that obtained previously by Utsumi (1985). We refer the reader to Paper II for the detailed discussion made there about the explanation of this difference.

[4] Because of the difficulties in deriving Sr abundances, we discard this element when computing the mean low-mass *s*-element abundances ls (see discussion in Paper II).

3. Tc AND POSSIBLE BINARITY

The radioactive nucleus ^{99}Tc ($\tau_{1/2} \sim 2 \times 10^5$ yr) is produced along the *s*-process path. Because the AGB phase spans only a few half-lives of this element, once dredged up into the envelope, it should remain present in a certain percentage throughout the AGB lifetime.

Therefore, the detection of Tc in the atmosphere of an AGB star (Merrill 1952) is undeniable evidence of the *s*-process working in situ (*intrinsic* AGB). When, on the contrary, Tc presence can be excluded, the star most probably owes its carbon enrichment to a mass transfer episode from an AGB companion, *extrinsic* AGB. Unfortunately, the detection of Tc in AGB stars is a difficult task. The most interesting Tc lines are located around $\lambda \approx 4260$ Å, where AGB stars are not very bright.

Indeed, in most N stars this spectral region is not accessible to observations because of the strong flux depression at these wavelengths. There are, however, a couple of intercombination Tc lines that may be used for the analysis. One of them is the Tc I λ5924.47 line, which is, however, weak and not free from blends. We have extended the analysis of Tc in N stars made in Paper II using this line in the additional stars included in this work. We have followed the same technique as described in Abia & Wallerstein (1998). In Table 5 we show the results of this search. As in Paper II, a "yes" entry in this table means that the best fit to the λ5924 blend is obtained with a nonzero Tc abundance. A

"no" entry means that a synthetic spectrum with no Tc does not significantly differ from another one with a small Tc abundance. Finally, a "doubtful" entry means that the λ5924 blend can be fitted better with a small abundance of Tc, but the Tc absorption in the blend is not so clearly appreciated as in the case of the Tc "yes" stars. If we consider the "doubtful" stars as yielding a detection, which is probably the case, Table 5 shows that about 62% of our targets are Tc-yes N stars and thus can be considered as bona fide intrinsic carbon stars. However, because of the difficulty in the analysis of this Tc line (weak and in a very crowded zone), a nondetection does not necessarily mean that Tc is absent: we do not have, unfortunately, a clear-cut possibility of excluding it. Probably, a study of the resonance lines at 4260 Å, when feasible, could yield more secure conclusions. Thus, additional tests are necessary to establish the extrinsic or intrinsic nature for the rest of the sample.

A further help can luckily come from an analysis of infrared colors. This idea (Jura 1986; Little-Marenin & Little 1988) arises from the fact that intrinsic AGB stars (in our case N stars) are high-mass losers and show excess infrared radiation from circumstellar dust, whereas extrinsic N stars would be first-ascent red giants with mass-loss rates smaller by at least 2 orders of magnitudes. This was already used by Jorissen et al. (1993) to distinguish between extrinsic and intrinsic S stars. These authors showed that the overwhelming majority of Tc-deficient S stars have a ratio $R = F(12\ \mu\mathrm{m})/F(2.2\ \mu\mathrm{m}) < 0.1$, where $F(12\ \mu\mathrm{m})$ and $F(2.2\ \mu\mathrm{m})$ are the 12 and 2.2 μm fluxes from the *IRAS* Point Source Catalog and from the Two Micron All Sky Survey, respectively. On the contrary, most Tc-rich S stars (intrinsic) have $R > 0.1$. We have performed a similar study in our sample of carbon stars, and the result can be seen in the histogram of Figure 3. We have considered in this plot the doubtful stars as showing Tc in their spectra because of the reasons commented above. From this figure it is obvious that most of our stars have infrared excess $R > 0.1$ and only a few show lower values (in fact, in the very narrow range $\sim$0.08–0.1). It is clear that, contrary to what happens for the S stars (see Jorissen et al. 1993), there is no distinction in the distribution between Tc-yes and Tc-no carbon stars. We might then conclude that probably all carbon stars in our sample are in fact of intrinsic nature and the quoted Tc-no carbon stars are just a consequence of the difficult and uncertain analysis of the Tc I λ5924 blend on which this study is based.[5]

Similarly to what happens in S stars, a difference between Tc-yes and Tc-no carbon stars might also be apparent in their temperature class. The large uncertainty in the derivation of the effective temperature in carbon stars does not allow us to address this question directly from the estimated T_{eff} values. The point is that Tc-yes carbon stars should be cooler and more evolved and hence should (on average) have more circumstellar matter to account for the infrared excess. This question can be addressed by studying the K–[12] versus K–[25] color-color diagram. The color index K–[i] is defined as $K - 2.5\log[620/F(i)]$, $F(i)$ being the (non–color-corrected) flux in the i band taken from the *IRAS* Point Source Catalog. Again, we do not find a distinction between Tc-yes and Tc-no stars (see Fig. 4). All the stars are located in the region of blackbodies with $T \lesssim 3000$ K. These temperatures are indeed expected in evolved stars during

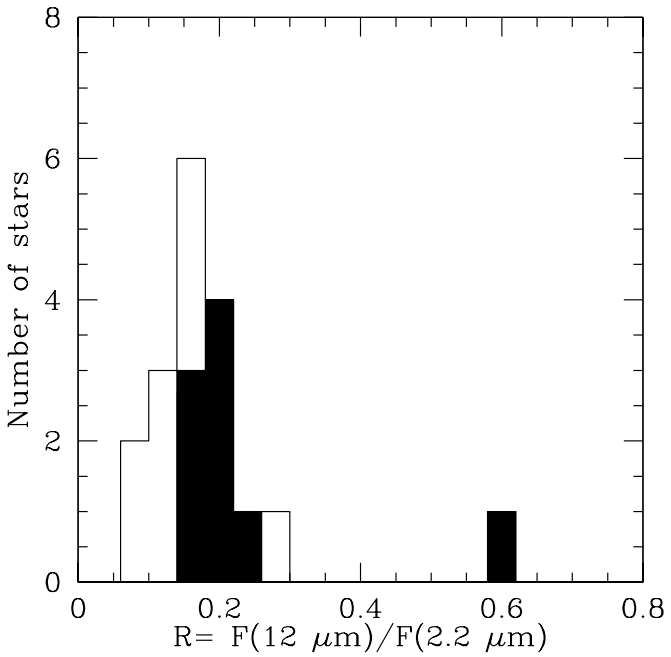

FIG. 3.—Distribution of $R = F(12\ \mu\mathrm{m})/F(2.2\ \mu\mathrm{m})$ for Tc-yes (*open histogram*) and Tc-no (*shaded histogram*) N stars. The Tc-no stars with $R > 0.6$ are collected in the last bin.

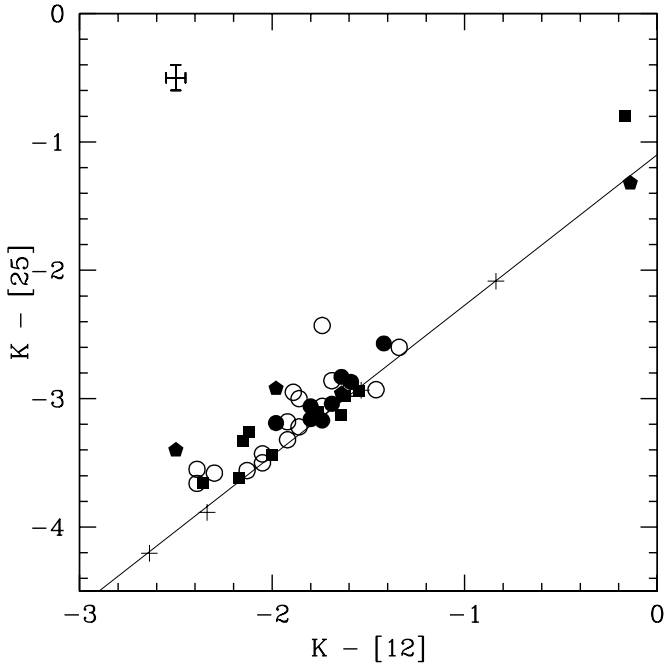

FIG. 4.—(K–[12], K–[25]) color-color diagram, where open circles stand for Tc-yes and filled circles for Tc-no N stars. Filled pentagons are stars in our sample with no information about Tc (whether from this work or the literature). Filled squares are the carbon stars of J type studied by Abia & Isern (2000). J stars do not show Tc. The solid line represents blackbody colors, with crosses corresponding to temperatures 4000, 3000, 2000, and 1500 K. The error bars represent a typical uncertainty of 5% and 10% on the 12 and 25 μm fluxes, respectively. Note that there is not any segregation between different groups of carbon stars in this diagram.

[5] Note that, as mentioned in Paper II, in some stars we were able to study simultaneously the stronger resonance Tc I λ4260 lines. In all the stars where this was possible, we confirmed the detection found from the λ5924 blend.

the AGB phase of evolution (note that some stars have blackbody temperatures lower than 2000 K). Higher blackbody temperatures would instead be expected in extrinsic (RGB) carbon stars.

A better discrimination will be possible in this field when extensive colors for C-rich and O-rich AGB stars from modern infrared cameras become available, providing data with a higher precision than possible from *IRAS* (see preliminary results by Marengo et al. 1999; Busso et al. 2001b).

Finally, we can also address the problem of the nature of our sample stars (i.e., those being extrinsic or intrinsic AGBs) through a comparison with theoretical models of element enrichment in the two classes of objects, to look for parameters helping in the discrimination. There are several questions for which we can, in this way, find useful answers. Is it possible, at nearly solar metallicity, to produce an extrinsic carbon star (C/O > 1) from the transfer of carbon-rich material in a binary system (most probably through the wind accretion mechanism; Jorissen & Mayor 1988)? What should be the C/O ratio in the transferred material so that the mass-receiving companion remains C-rich? How much do these requirements depend on the stellar mass and on the metallicity of the accreting star and of the donor? We shall revisit these problems in the next section, where we present a comparison of our observations with the results of nucleosynthesis and mixing models for intrinsic and extrinsic AGB stars.

4. COMPARISON WITH MODELS OF AGB NUCLEOSYNTHESIS

In order to understand the way in which the observed abundances were created and subsequently mixed into the stellar convective envelopes, we made use of the same stellar and nucleosynthesis models already described in Paper II. They start from full stellar evolution calculations, computed with the FRANEC evolutionary code, spanning the metallicity range from solar to 1/20 solar and the mass range from 1.5 to 7 $M_{\odot}$ (Straniero et al. 1997, 2000).

For our purposes, we adopt the 1.5 $M_{\odot}$ model as representative of LMSs, since in Paper II we already concluded that most N stars are of low mass ($M \lesssim 3\ M_{\odot}$). Notice that the theoretical expectations for a 3 $M_{\odot}$ stellar model mimic quite closely the 1.5 $M_{\odot}$ model: differences in *s*-element logarithmic abundances are found to be below 0.1 dex. We have computed models without mass loss, from which an asymptotic value of the parameter $\lambda = \Delta M(\mathrm{TDU})/\Delta M_{\mathrm{H}}$ has been derived, namely, 0.24 for the 1.5 $M_{\odot}$ model. On this basis a postprocessing has been performed to derive the detailed nucleosynthesis products in the He intershell and the chemical modifications of the envelope (Gallino et al. 1998). The duration of the thermally pulsing AGB phase is mainly determined by the assumed mass-loss rate. Hence, mass loss was included in the nucleosynthesis calculations through the Reimers (1975) phenomenological law, choosing the value 0.7 for the free parameter η. In each interpulse/pulse cycle we compute the detailed nucleosynthesis pattern that is established in the intershell zone, induced first by the neutron release from radiative ^{13}C burning in the interpulse phase and then by the activation of the ^{22}Ne neutron source in the convective instability of the He shell. One cycle after the other, we follow the penetration of envelope convection through TDU that mixes part of the processed material to the envelope; the whole sequence is repeated until our models experience the end of TDU. The procedure assumes that some form of proton penetration below the convective border can occur at dredge-up, polluting the radiative He- and C-rich layers, so that at the restart of H shell burning the main neutron source ^{13}C can be formed. For the problems and the uncertainties involved in this assumption, as well as for the techniques used in the computations of neutron captures and the nuclear parameters used, see Paper II and Gallino et al. (1998). There, in particular, we described the way in which our model sequences are created and the efficiency of ^{13}C burning assumed. As in Paper II, we shall refer with the term ST (*standard*) to models in which the mass of ^{13}C burned per cycle is $4 \times 10^{-6}\ M_{\odot}$ in LMSs. Then this reference abundance is scaled upward and downward to span a wide range of possibilities in the nucleosynthesis efficiency, from a maximum of ST×2 down to a minimum of ST/12, as it was done in Paper II.

Figures 5, 6, and 7 show a synthesis of our predictions:[6] they present, as a function of the initial metallicity [M/H], the average photospheric abundance ratios [hs/M], [ls/M], and [hs/ls] at C/O = 1, in our 1.5 $M_{\odot}$ model, assumed as representative of the LMS class.

Inspection of Figures 5, 6, and 7 provides a quite satisfactory agreement between observations and theoretical models, inside the wide spread of neutron release efficiency considered and taking into account the observational uncertainties of N stars. This is in agreement with previous findings on the average *s*-process efficiency by Busso et al. (2001a), derived by other classes of AGB stars and their descendants at various metallicities.

[6] Stellar models were computed with an oxygen enhancement assuming the relationship [O/Fe]≈ −0.4[Fe/H].

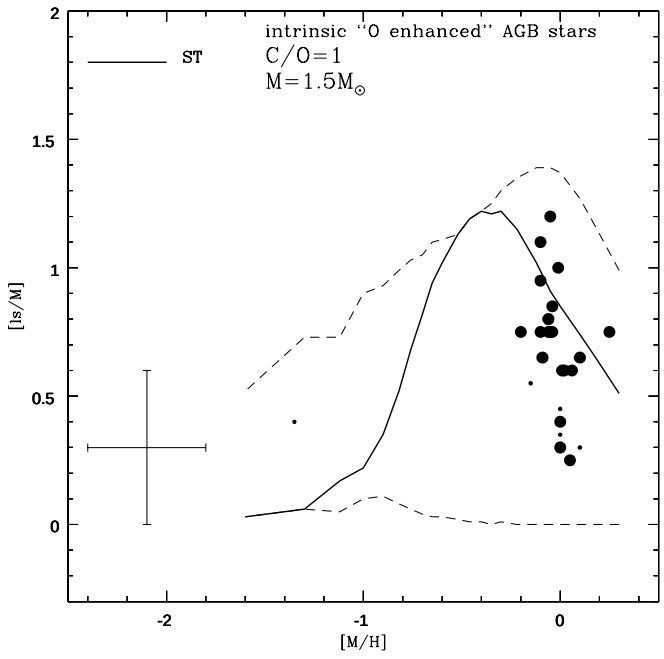

FIG. 5.—Comparison of the observed mean low-mass *s*-element (Y, Zr) [ls/M] enhancement against metallicity with theoretical predictions for a 1.5 $M_{\odot}$ TP-AGB star. The theoretical predictions shown are for O-enhanced stellar models at C/O = 1. The upper and lower curves (*dashed lines*) limit the region allowed by the models according to the different ^{13}C pocket choices (see text). Note that several stars coincide in the same data point. The *difficult* stars are plotted with smaller symbols (see Paper II).

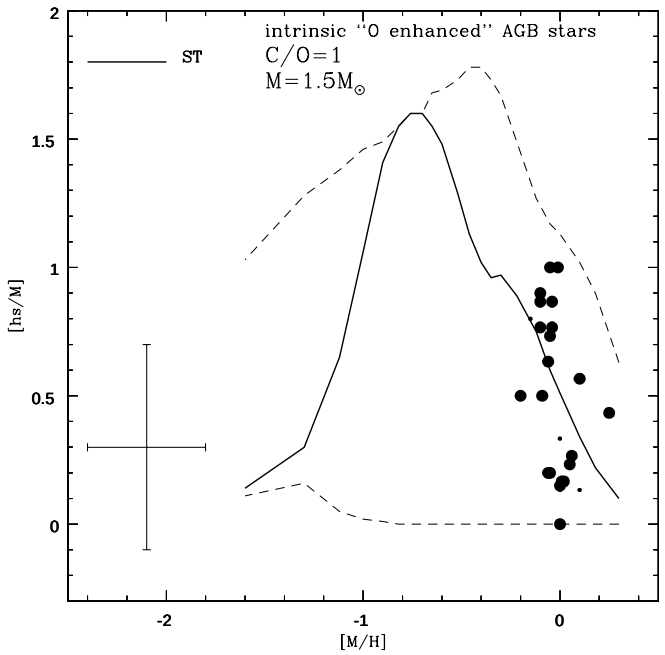

FIG. 6.—Same as Fig. 5, but for the observed mean high-mass *s*-element (Ba, La, Nd) [hs/M] enhancement as compared with theoretical predictions for a 1.5 $M_{\odot}$ TP-AGB star.

A rather comprehensive picture of the *s*-enrichment in N stars is provided by plots in which observations and theory are compared using the *s*-element enhancement (indicated by, e.g., ls) and a parameter sensitive to the neutron exposure (e.g., [hs/ls], as shown in Busso et al. 1995, 2001a). This kind of comparison is performed in Figure 8, where N stars are shown together with other known classes of intrinsic and extrinsic AGB stars. As the figure shows, the spread in the *s*-process efficiency, as monitored by the N(^{13}C)/N(^{56}Fe) ratio in the pocket, is in this way constrained better, being rather limited. Another result is that N stars are very close to S stars for what concerns the efficiency of mixing into the envelope. In the models, it is indeed often sufficient to make one extra pulse to change the composition of an S star into that of an N giant, establishing a C/O ratio larger than unity. This has large consequences on the appearance of the atmosphere and of the circumstellar envelope (chemistry, colors, and type of dust formed all change considerably), but the corresponding change in the *s*-process enhancement may be rather limited. Since post-AGB stars usually show larger *s*-element enhancements than those derived here in N stars (see § 1), and because our sample stars show a C/O ratio very close to 1, we might speculate that the stars analyzed here have just become carbon stars. As the star evolves in the AGB phase and TPs and TDUs continue operating, more carbon and *s*-elements are dredged up into the envelope. Eventually the C/O ratio exceeds unity by such a large amount that the star becomes obscure at optical wavelengths as a result of the formation of dust. This scenario might explain the apparent *gap* in the level of *s*-element enhancement and C/O ratio observed between C(N) stars and post-AGB stars: we cannot "see" carbon stars with a C/O ratio largely exceeding unity. We have to outline once again that our conclusions are for the moment somewhat hampered by the still large observational uncertainties for N stars, whereas typical error bars for the other classes of *s*-enriched stars in the Galactic disk are in general lower (0.20–0.25 dex; see, e.g., Busso et al. 2001a).

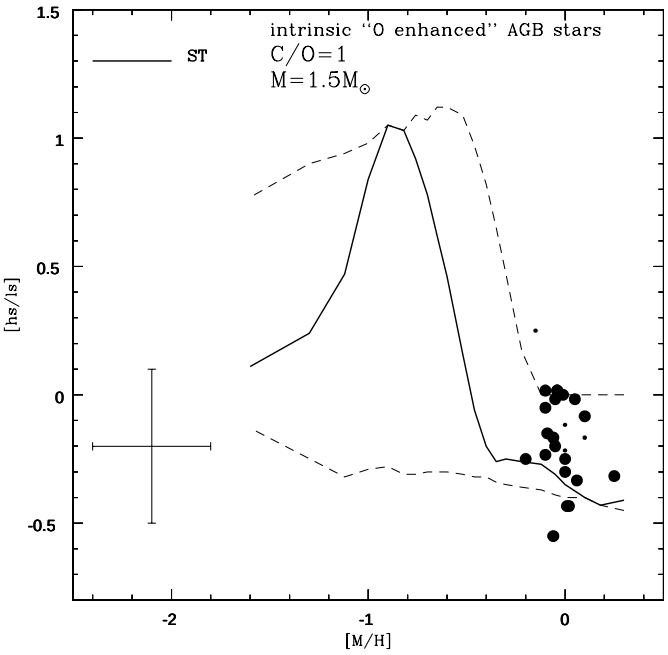

FIG. 7.—Same as Fig. 5, but for the observed mean [hs/ls] ratio (signature of the neutron exposure) as compared with theoretical predictions for a 1.5 $M_{\odot}$ TP-AGB star.

The interpretation of the N star abundances presented so far in the framework of LMS evolution along the AGB is confirmed, and even strengthened, by an analysis of the detailed element distributions in the observed stars, from the data of Table 5. In order to show this, we have plotted in Figure 9 a sample of fits to individual stars, obtained by comparing their observed composition with that yielded by the models in the photosphere, at C/O = 1. The plots show a satisfactory agreement, and we believe that this provides a full confirmation that most, if not all, N stars of the Galactic disk are indeed of low initial mass. In fact, from the discussion presented in Paper II we know a priori that plots made similarly to Figure 9, but using models from IMSs, would often be incapable of reproducing at least the "ls" zone, yielding in general a too high Rb/Sr ratio. This conclusion for the mass of carbon stars is in line with the present independent understanding of the different classes of carbon stars, provided by astrometric, kinematic, and photometric criteria (Bergeat et al. 2002a, 2002b).

4.1. *Can Any of Our Sources Be an Extrinsic C Star?*

Using the models outlined in the previous subsection, we can add something to the discussion of the nature of our sources. This can be done on an independent basis with respect to the (already analyzed) presence of Tc and infrared properties. Having in mind the model compositions discussed above, we can ask ourselves which predictions for *s*-element and carbon abundances would be derived in case some of our sample stars were extrinsic AGBs. In order to study this possibility, we have first to consider that the resulting C/O ratio after mass transfer is constrained by the observed C/O value, which is very close to 1. Then we must take into account the original C and O content in the companion. This depends on metallicity, and at the moment of

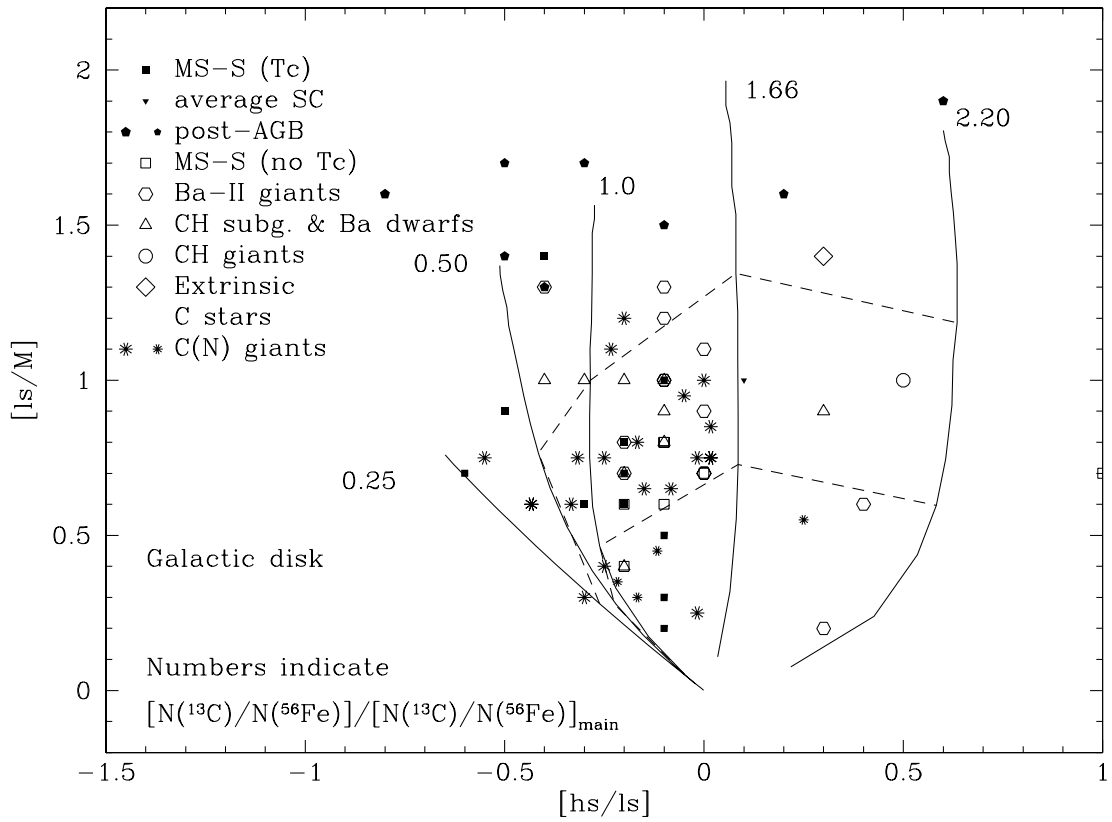

FIG. 8.—Observed trend of the ls element abundances [ls/M] vs. [hs/ls] for Galactic disk intrinsic and extrinsic AGB stars. The solid curves refer to envelope models with different *s*-process efficiency, as monitored by the $N(^{13}C)/N(^{56}Fe)$ ratio (here normalized to the case that fits the main component in the solar system). The dashed lines connect the points corresponding to the fourth and eighth dredge-up episode to make clear how the stars distribute along the TP-AGB evolutionary sequence. Difficult N and post-AGB stars have been plotted with smaller symbols.

mass transfer it has probably not changed from the original CNO composition. Indeed, the long duration of core H burning (which precedes any significant abundance change at the surface) makes this phase the most likely for the occurrence of mass accretion. Subsequently, partial ^{12}C depletion is produced by the first dredge-up (FDU), during the RGB phase; FDU also increases the abundance of ^{13}C (^{16}O is only slightly reduced by FDU).

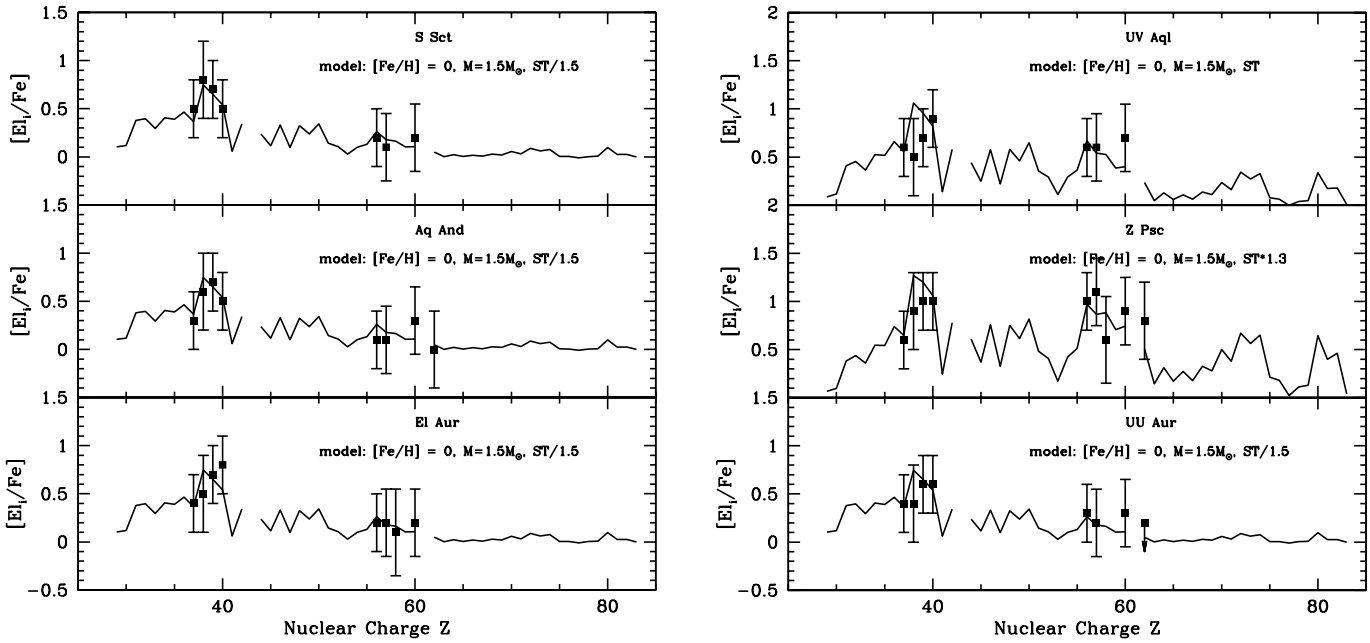

FIG. 9.—Detailed reproduction of the observed abundances in the carbon stars S Sct, AQ And, EL Aur (*left panel*), UV Aql, Z Psc, and UU Aur (*right panel*). The labels indicate the stellar mass model and metallicity that better fits the abundances of a given star together with the choice of the ^{13}C burned per cycle referred to the standard case (ST). See text for details.

For a star reaching the RGB with a solar mixture of CNO isotopes, FDU would change CN abundances by a significant fraction (e.g., ^{12}C would decrease by 13%–40% in solar metallicity models spanning the range 1–5 $M_{\odot}$). Its impact is, however, marginal when the star has a high carbon enhancement at the surface. Furthermore, in case of a lower than solar metallicity, one must take into account that the initial carbon abundance decreases with Fe, whereas [O/Fe] shows a concomitant enhancement. One can adopt general rules for this enhancement, deducing it from observations of large databases of dwarf stars at different metallicities, e.g., as described in Israelian et al. (2001). Note that while [O/Fe] versus [Fe/H] still remains controversial at [Fe/H] < -1, this does not affect our discussion because the typical metallicity of our sample stars is much higher.

We then modeled mass transfer by diluting the AGB envelope composition, allowing for different "mixing histories," which take into account the different possibilities described above. In all our attempts we found that, for metallicities not far from solar, it is impossible to produce an extrinsic carbon star. This gives a strong support to the indications already obtained from the observational criteria.

To make this result easily understood, we can express the mass transferred by means of a semianalytic formula. If mass transfer occurs while the secondary component is on the main sequence, the material accumulates onto a thin radiative region, whose chemical composition becomes that of the accreted material from the AGB companion and is therefore characterized by a C/O ratio in excess of unity. At FDU, a homogeneous composition is established by mixing the accreted material over more internal layers, where the original chemical composition, partly modified by H burning, has been preserved. Then, we can define a dilution factor f as the ratio of the transferred mass ($M_{\rm AGB}^{\rm tr}$) to the fraction of the envelope having the original composition ($M_{\rm comp}^{\rm env,ini}$). By imposing that, in the photosphere of the secondary star, the C/O ratio remains equal to 1 even after FDU, one can see that

$$f = \left(1 - \frac{0.28}{10^{-0.4[\mathrm{Fe/H}]}}\right)\left[\left(\frac{\mathrm{C}}{\mathrm{O}}\right)_{\rm AGB}^{\rm lastTDU} - 1\right]^{-1}.$$

Here we have assumed that mass transfer occurs at the last TDU episode, in order to allow the maximum possible carbon enhancement of the secondary component, thus favoring the formation of an extrinsic carbon star. According to the FRANEC models, TDU ceases when the envelope mass drops below a critical limit, namely, $\sim$0.5 $M_{\odot}$; from then on, while mass loss can further decrease the envelope mass, its C/O ratio remains frozen. In Table 6 we report, for the 1.5 $M_{\odot}$ model at different metallicities (first column), the final C/O ratio of the intrinsic AGB star (primary component) at the last thermal pulse that experienced TDU [$(\mathrm{C/O})_{\rm AGB}^{\rm lastTDU}$] and the corresponding dilution ratio f, as derived by means of the formula reported above. Obviously, there is a maximum limit in the transferred mass, which corresponds to the accretion of the whole residual mass of the AGB envelope (i.e., $\sim$0.5 $M_{\odot}$). In order to give an estimate for such a limit, we further assumed that the mass of the companion star, after the mass accretion, is the lowest compatible with the age of the Galactic disk, say, $\sim$1 $M_{\odot}$. Again, this is intended to favor carbon enrichment, as it roughly corresponds to the minimum mass of the convective envelope at the FDU. Correspondingly, in the most favorable conditions, we obtain an upper limit for the dilution factor f of 1.5. We emphasize that this limit corresponds to a very extreme case, and we expect that a substantially lower value of the f parameter should be more realistic. For example, if the mass of the secondary component after the mass accretion episode were 1.5 $M_{\odot}$ (corresponding to an initial mass of about 1 $M_{\odot}$), the limiting value of the f parameter would become 0.7. In any case, from a comparison with the calculated f-values reported in Table 6, it is clear that it would be practically impossible to form extrinsic carbon stars for solar metallicities. We suggest that the maximum metallicity of an extrinsic carbon star should be of the order of [Fe/H] ~ -0.4 to -0.3.

TABLE 6

PREDICTED C/O RATIO AND f-VALUE IN EXTRINSIC AGB STARS

	1.5 $M_{\odot}$	
[Fe/H]	$(\mathrm{C/O})_{\rm AGB}^{\rm lastTDU}$	f
0.00	1.45	1.60
−0.12	1.65	1.15
−0.30	2.00	0.79
−0.40	4.28	0.25
−0.52	5.02	0.21
−0.60	5.55	0.18
−0.70	6.28	0.16
−0.82	7.36	0.14
−1.00	9.18	0.11
−1.30	13.29	0.07
−1.60	33.08	0.03

Thus, even considering the uncertainty in the metallicity of the stars considered in the present work ($\pm$0.3 dex), this simple result prevents the vast majority of them from being considered as extrinsic carbon stars.

Note that if a carbon star is formed as a consequence of the mass transfer process, as is indeed the case at lower metallicities, then the behavior of [ls/Fe] versus [Fe/H] would not be distinguishable from the trend seen for intrinsic AGBs. This is related to the fact that mass transfer and the following FDU behave much like a form of dilution, as in the case of TDU, and we have no way to distinguish which of the two possible forms of dilution the *s*-enriched material has undergone (see Busso et al. 2001a, in particular their Figs. 11 and 12, for a discussion of this in the case of Ba and CH stars).

In conclusion, both the observational and theoretical analyses lead us to conclude that the objects studied here are most probably intrinsic carbon stars, presently evolving along the TP-AGB. Exceptions may exist, but this should be tested with more direct methods, like radial velocity variations and their effects on the spectra. At the moment, for none of the N stars studied here is there any evidence of such variations.

5. CONCLUSIONS

In this paper we have presented for the first time a rather complete sample of *s*-process abundance measurements in N-type carbon stars, extended to light and heavy species, across the *s*-process peaks with neutron numbers $N = 50$ and 82. Making use of a large line list and up-to-date model

atmospheres for carbon-rich giants, we have deduced the *s*-element abundances through the spectrum synthesis technique. In doing so, we have also verified previous results (Paper II) for the light *s*-elements across the ^{85}Kr branching point of the *s*-path. N stars turn out to be characterized by s-element abundances very close to, or slightly higher than, those found for S stars. Compared with the only analysis performed before (Utsumi 1985), our abundances are clearly smaller; they are smaller also with respect to those of post-AGB supergiants (Reddy, Bakker, & Hrivnak 1999; Van Winckel & Reyniers 2000), and this gives rise to a general picture in which the surface enrichment continuously increases along the evolutionary sequence producing MS, S, and N stars and subsequently yellow post-AGB supergiants (Reddy et al. 2002). We have compared our data with model envelope compositions obtained from previously published calculations of AGB nucleosynthesis and mixing. Good agreement is obtained between LMS models and *s*-element observations. Several pieces of evidence (from the detection of Tc lines and infrared colors to the theoretical relations between the initial metallicity, the mass, and the final C/O ratio) lead us to conclude that most (or perhaps all) of our sample stars are intrinsic TP-AGB stars, so that their abundances are locally produced by the occurrence of third dredge-up during the TP-AGB phases and not generated by mass transfer in binary systems.

Data from the VALD database at Vienna were used for the preparation of this paper. K. Eriksson and the stellar atmosphere group of the Uppsala Observatory are thanked for providing the grid of atmospheres. The 4.2 m WHT and the 2.5 m NOT are operated on the island of La Palma by the RGO in the Spanish Observatory of the Roque de los Muchachos of the Instituto de Astrofísica de Canarias. This work was also based in part on observations collected with the 2.2 m telescope at the German-Spanish Astronomical Centre, Calar Alto. It was partially supported by the Spanish grants AYA2000-1574 and FQM-292, by the Italian MURST-Cofin2000 project "Stellar Observables of Cosmological Relevance," and by the French-Spanish International Program for Scientific Collaboration, PICASSO HF2000-0087.

REFERENCES

Abia, C., Busso, M., Gallino, R., Domínguez, I., Straniero, O., & Isern, J. 2001, ApJ, 559, 1117 (Paper II)
Abia, C., & Isern, J. 2000, ApJ, 536, 438
Abia, C., & Wallerstein, G. 1998, MNRAS, 293, 89 (Paper I)
Alkniss, A., Balnauss, A., Dzervitis, V., & Eglitis, I. 1998, A&A, 338, 209
Anders, E., & Grevesse, N. 1989, Geochim. Cosmochim. Acta, 53, 197
Arenou, F., Grenon, M., & Gómez, A. 1992, A&A, 258, 104
Bard, D. J., Barisciano, L. P., & Cowley, C. R. 1996, MNRAS, 278, 997
Barnbaum, C., Stone, R. P. S., & Keenan, P. C. 1996, ApJS, 105, 419
Bauschlicher, C. W., Langhoff, S. R., & Taylor, P. R. 1988, ApJ, 332, 531
Beer, H., & Macklin, R. L. 1989, ApJ, 339, 962
Bergeat, J., Knapik, A., & Rutily, B. 2001, A&A, 369, 178
———. 2002a, A&A, 385, 94
———. 2002b, A&A, 390, 987
Beveridge, R. C., & Sneden, C. 1994, AJ, 108, 285
Busso, M., Gallino, R., & Wasserburg, G. J. 1999, ARA&A, 37, 239
Busso, M., Lambert, D. L., Beglio, L., & Gallino, R. 1995, ApJ, 446, 775
Busso, M., Lambert, D. L., Gallino, R., Travaglio, C., & Smith, V. V. 2001a, ApJ, 557, 802
Busso, M., Marengo, M., Travaglio, C., Corcione, L., & Silvestro, G. 2001b, Mem. Soc. Astron. Italiana, 72, 309
Cardelli, J. A., Clayton, G. C., & Mathis, J. S. 1989, ApJ, 345, 245
Cerny, D., Bacis, R., Guelachvili, G., & Roux, F. 1978, J. Mol. Spectrosc., 73, 154
Claussen, M. J., Kleinmann, S. G., Joyce, R. R., & Jura, M. 1987, ApJS, 65, 385
de Laverny, P., & Gustafsson, B. 1998, A&A, 332, 661
Dominy, J. 1985, PASP, 97, 1104
Dyck, H. M., van Belle, G. T., & Benson, J. A. 1996, AJ, 112, 294
Epchtein, N., et al. 1999, A&A, 349, 236
Eriksson, K., Gustafsson, B., Jørgensen, U., & Nordlund, A. 1984, A&A, 132, 37
Gallino, R., Arlandini, C., Busso, M., Lugaro, M., Travaglio, C., Straniero, O., Chieffi, A., & Limongi, M. 1998, ApJ, 497, 388
Gezari, D. Y., Pitts, P. S., & Schmitz, M. 1999, Catalog of Infrared Observations, electronic release at the SIMBAD database (5th ed.; Strasbourg: CDS)
Groenewegen, M. A. T., Whitelock, P. A., Smith, C. H., & Kerschbaum, F. 1998, MNRAS, 293, 18
Gustafsson, B., & Jørgenssen, U. G. 1994, A&A Rev., 6, 19
Holweger, H., & Müller, E. A. 1974, Sol. Phys., 39, 19
Iben, I., Jr., & Renzini, A. 1983, ARA&A, 21, 271
Israelian, G., Rebolo, R., García López, R., Bonifacio, P., Molaro, P., Basri, G., & Shchukina, N. 2001, ApJ, 551, 833
Ito, H., Ozaki, Y., Suzuki, K., Kondow, T., & Kuchitsu, K. 1988, J. Mol. Spectrosc., 127, 283
Jørgensen, U. G., Larsson, M., Iwamae, A., & Yu, B. 1996, A&A, 315, 204
Jorissen, A., Frayer, D. T., Johnson, H. R., Mayor, M., & Smith, V. V. 1993, A&A, 271, 463
Jorissen, A., & Mayor, M. 1988, A&A, 198, 187
Jura, M. 1986, Irish Astron. J., 17, 322
Kilston, S. 1975, PASP, 87, 189
Kipper, T. 1998, Baltic Astron., 7, 435
Knapp, G. R., & Morris, M. 1985, ApJ, 292, 640
Knapp, G. R., Pourbaix, D., & Jorissen, A. 2001, A&A, 371, 222
Kotlar, A. J., Field, R. W., & Steinfeld, J. I. 1980, J. Mol. Spectrosc., 80, 86
Kupka, F., Piskunov, N., Ryabchikova, T. A., Stempels, H. C., & Weiss, W. W. 1999, A&AS, 138, 119
Kurucz, R. L. 1993, CD-ROM 1–23, Data Bank (Cambridge: SAO)
Lambert, D. L., Gustafsson, B., Eriksson, K., & Hinkle, K. H. 1986, ApJS, 62, 373
Larsson, M., Siegbahn, P. E. M., & Ågren, H. 1983, ApJ, 272, 369
Little-Marenin, I. R., & Little, S. J. 1988, ApJ, 333, 305
Lloyd-Evans, T. L. 1983, MNRAS, 204, 945
Luck, R. E., & Bond, H. E. 1991, ApJS, 77, 515
Luque, J., & Crosley, D. R. 1999, SRI International Rep. MP 99-009
Marengo, M., Busso, M., Persi, P., Silvestro, G., & Lagage, P. O. 1999, A&A, 348, 501
Marengo, M., Ivezic, Z., & Knapp, G. R. 2001, MNRAS, 324, 1117
McWilliam, A. 1998, AJ, 115, 1640
Meggers, W. F., Corliss, C. H., & Scribner, B. F. 1975, NBS Monograph 145
Merrill, P. W. 1952, ApJ, 116, 21
Neugebauer, G., & Leighton, R. B. 1969, Two Micron All Sky Survey, NASA SP-3047 (TMSS)
Nollett, K. M., Busso, M., & Wasserburg, G. 2002, ApJ, in press
Ohnaka, K., & Tsuji, T. 1996, A&A, 310, 933
Olofsson, H., Eriksson, K., Gustafsson, B., & Carlstrom, U. 1993, ApJS, 87, 267
Paczyński, B. 1970, Acta Astron., 20, 47
Piskunov, N. E., Kupka, F., Ryabchikove, T. A., Weiss, W. W., & Jeffry, C. S. 1995, A&AS, 112, 525
Plez, B. 1998, A&A, 337, 495
Pourbaix, D., Knapp, G. R., & Jorissen, A. 2002, A&A, submitted
Prasad, C. V. V., & Bernath, P. F. 1992, J. Mol. Spectrosc., 156, 327
Prasad, C. V. V., Bernath, P. F., Frum, C., & Engleman, R., Jr. 1992, J. Mol. Spectrosc., 151, 459
Reddy, B. E., Bakker, E. J., & Hrivnak, B. J. 1999, ApJ, 524, 831
Reddy, B. E., Lambert, D. L., Gonzalez, G., & Yong, D. 2002, ApJ, 564, 482
Rehfuss, B. D., Suh, M. H., & Miller, T. A. 1992, J. Mol. Spectrosc., 151, 43
Reimers, D. 1975, in Problems in Stellar Atmospheres and Envelopes, ed. B. Bascheck, H. Kegel, & G. Traving (Berlin: Springer), 229
Schwarzschild, M., & Härm, R. 1965, ApJ, 142, 855
Skrutskie, M. F., et al. 1997, in The Impact of Large Scale Near-Infrared Surveys, ed. F. Garzon et al. (Dordrecht: Kluwer), 25
Smith, V. V., & Lambert, D. L. 1985, ApJ, 294, 326
———. 1986, ApJ, 311, 843
———. 1990, ApJS, 72, 387
Straniero, O., Chieffi, A., Limongi, M. Busso, M., & Gallino, R. 1997, ApJ, 478, 332
Straniero, O., Gallino, R., Busso, M., Chieffi, A., Raiteri, C., Salaris, M., & Limongi, M. 1995, ApJ, 440, L85
Straniero, O., Limongi, M., Chieffi, A., Domínguez, I., Busso, M., & Gallino, R. 2000, Mem. Soc. Astron. Italiana, 71, 719
Thévenin, F. 1989, A&AS, 77, 137
———. 1990, A&AS, 82, 179
Tomkin, J., & Lambert, D. L. 1983, ApJ, 273, 722

Utsumi, K. 1970, PASJ, 22, 93
———. 1985, in Cool Stars with Excesses of Heavy Elements, ed. M. Jascheck & P. C. Keenan (Dordrecht: Reidel), 243
van Leeuwen, F., & Evans, D. W. 1998, A&AS, 130, 157
Vanture, A. D. 1992a, AJ, 103, 2035
———. 1992b, AJ, 104, 1986
———. 1992c, AJ, 104, 1997
Van Winckel, H., & Reyniers, C. 2000, A&A, 354, 135
Wallerstein, G., & Knapp, G. R. 1998, ARA&A, 36, 369
Wallerstein, G., et al. 1997, Rev. Mod. Phys., 69, 995
Wasserburg, G. J., Boothroyd, A. I., & Sackmann, I.-J. 1995, ApJ, 440, L101
Westerlund, B. E., Azzopardi, M., Breysacher, J., & Rebeirot, E. 1991, A&A, 244, 367
———. 1995, A&A, 303, 107